J. Physiol. (1984). **354**, *pp.* 557–575
With 9 text-figures
Printed in Great Britain

THE CALCIUM CURRENT IN INNER SEGMENTS OF RODS FROM THE SALAMANDER (*AMBYSTOMA TIGRINUM*) RETINA

BY D. P. COREY, J. M. DUBINSKY AND E. A. SCHWARTZ

From the Department of Physiology, Yale University School of Medicine, New Haven, CT 06510, U.S.A., Department of Physiology, University of North Carolina, Chapel Hill, NC 27514, U.S.A. and the Department of Pharmacological and Physiological Sciences, The University of Chicago, Chicago, IL 60637, U.S.A.

(*Received 25 October 1983*)

SUMMARY

1. Solitary rod inner segments were isolated from salamander retinae. Their Ca current was studied with the 'whole-cell, gigaseal' technique (Hamill, Marty, Neher, Sakmann & Sigworth, 1981). The soluble constituents of the cytoplasm exchanged with the solution in the pipette. The external solution could be changed during continuous perfusion. Membrane voltage was controlled with a voltage clamp.

2. After permeant ions other than Ca were replaced with impermeant ions (i.e. tetraethylammonium as a cation, and aspartate or methanesulphonate as an anion), an inward current remained. It activated at approximately −40 mV, reached a maximum at approximately 0 mV, and decreased as the membrane was further depolarized. The size of the current increased when Ba was substituted for external Ca. The current was blocked when Ca was replaced with Co.

3. The voltage at which the current was half-maximum shifted from approximately −22 to −31 mV during the initial 3 min of an experiment. The maximum amplitude of the current continuously declined during the entire course of an experiment.

4. The time course for activation of the Ca current following a step of depolarization could be described by the sum of two exponentials. The time constant of the slower exponential was voltage dependent. Deactivation following repolarization could also be described by the sum of two exponentials. Both time constants for deactivation were independent of voltage (between −30 and 0 mV) and faster than the slower time constant for activation.

5. When the internal Ca concentration was buffered by 10 mM-EGTA, the Ca current did not inactivate during several seconds of maintained depolarization.

6. When the concentration of EGTA was reduced to 0·1 mM, the Ca current declined and the membrane conductance decreased during several seconds of maintained depolarization. This inactivation was incomplete and only occurred after a substantial quantity of Ca entered. Following repolarization the Ca conductance recovered from inactivation. In contrast, the continuous decline observed during the course of an experiment (item 3) was not reversible. The difference suggests that inactivation and the decline are distinct processes.

INTRODUCTION

The signal produced by light in a rod outer segment spreads to the inner segment where it is modified by the collaborative action of five currents (Bader, Bertrand & Schwartz, 1982). One of these is a Ca current which also, presumably, regulates exocytosis. Rods do not normally produce action potentials; their release of transmitter is graded with the continuous polarization produced by light (see review by Schwartz, 1982). The smallest signal, the absorption of one photon, produces only a 30 μV transient hyperpolarization (Schwartz, 1975; Copenhagen & Owen, 1976). Because this signal can be relayed to post-synaptic neurones (Hecht, Shlaer & Pirenne, 1942; see also Ashmore & Falk, 1980), the rod synapse must have properties which assure reliable communication for very small presynaptic voltage changes. Study of the Ca current may reveal its role in achieving this excellent performance. Furthermore, its behaviour may serve as a model for Ca currents controlling exocytosis in other non-spiking neurones of the vertebrate central nervous system.

A preliminary description of the Ca current has been obtained using a single-micropipette voltage clamp (Bader *et al.* 1982). We extended the description using the patch-clamp method for recording whole-cell currents (Hamill, Marty, Neher, Sakmann & Sigworth, 1981). This method has two advantages. First, exchange of the pipette solution with the cytoplasm allows other inner segment currents to be suppressed and the Ca current to be studied in isolation. Secondly, temporal resolution is improved more than tenfold, allowing measurement of the time course of current activation and deactivation.

METHODS

Experiments were performed on salamanders, *Ambystoma tigrinum*, which were in their aquatic phase. The procedure for dissociating the retina and maintaining solitary photoreceptors was similar to that described previously (Bader, MacLeish & Schwartz, 1978). Briefly, an eye was hemisected and a square of absorbent paper was wetted to the posterior half. The retina adhered to the paper and could then be lifted from the underlying pigment epithelium. Retinae were incubated in saline (Table 1, solution A) with added papain (7 u./ml; Worthington no. 3126) for 10–14 h at 18 °C. Afterwards, they were transferred to 1 ml saline without enzyme and gently triturated. A drop of the resulting cell suspension was placed on a cover-slip in an otherwise empty Petri dish. The cover-slips were either plastic (Lux, no. 5407), or glass coated with collagen (Collagen Corp., Vitrogen 100), or glass coated with poly-DL-ornithine. After 30 min, the Petri dishes containing the cover-slips were filled with saline. Cells were kept for up to 3 weeks at 12 °C in a moist, oxygen atmosphere. Electrophysiological experiments were performed after a cover-slip was transferred to a chamber of 0·3 ml volume which could be continuously perfused at 1 ml/min. A change in solution was 99 % complete in less than 2 min. Solutions (see Table 1) were cooled with a Peltier device; the bath temperature was measured with a thermocouple probe (Bailey Instruments, IT-18) positioned a few millimetres from the cells.

Rod inner segments (inclusive of the nuclear region) were identified by their prominent ellipsoid and distinguished from cone inner segments by their more spherical shape. Most inner segments had fine calyceal processes at one pole, and a synaptic pedicle extending several micrometres from the other pole. For those cells apparently lacking a pedicle, it was not clear whether the pedicle was missing, was obscured from view by the soma, or had been resorbed. When cells were plated on coated glass cover-slips, a larger proportion of cells had a visible pedicle immediately after plating than several hours later, suggesting that resorption did occur.

The procedures for making pipettes, sealing a pipette to the surface of a cell, and recording were similar to those described by Hamill *et al.* (1981) and Corey & Stevens (1983). Recording pipettes

were drawn from 1·7 mm borosilicate capillary glass (Rochester Scientific, Boralex 100 μl). The internal tip diameter was approximately 0·5 μm after fire polishing. Pipettes filled with solution E or F had a resistance of 15–35 MΩ. Pipettes were coated to within 100 μm of their tips with Q-Dope (GC Electronics, no. 10-3702) or Sylgard (Dow Corning, no. 184). The increase in effective wall thickness reduced the capacitance to the bath.

The solution in the bath was electrically connected to the ground of the amplifier by a salt bridge containing 3% (w/v) agar and 100 mM-tetraethylammonium (TEA) Cl in series with a chlorided silver wire. A pipette was connected in a similar manner to the headstage of the voltage clamp, which was a current-to-voltage converter constructed from a FET-input operational amplifier

TABLE 1. Composition of solutions (mM)

	External solutions				Internal solutions	
	A	B	C	D	E	F
NaCl	90	—	—	—	—	—
KCl	2·5	—	—	—	—	—
TEA OH	—	100	100	100	100	100
D-aspartic acid	—	—	—	100	75	100
CH_3SO_3H	—	100	100	—	—	—
$CaCl_2$	3	—	—	—	—	—
$CaSO_4$	—	6	—	6	*	—
$CoSO_4$	—	—	6	—	—	—
$MgSO_4$	0·5	—	—	—	—	—
EGTA	—	—	—	—	10	0·1
HEPES	2	1	1	1	1	1
D-glucose	10	—	—	—	—	—

* The free Ca concentration in EGTA-buffered solutions was adjusted to 10^{-8} M as calculated from a dissociation constant of $1{\cdot}48 \times 10^{-7}$ M at pH 7·2 (Sillen & Martell, 1971).

All solutions contained 0·0025% (w/v) phenol red and were adjusted to pH 7·2–7·3 with NaOH (solution A) or TEA OH (solutions B–F). Solution A also contained 2% of an amino acid mixture (GIBCO no. 320–1130) and 5-fluorouracil 33 μg/ml to inhibit bacterial growth.

(either Burr-Brown 3523 or OPA 101) and a 200 MΩ feed-back resistor. Junction potentials between the ground and the input were nulled by an offset sufficient to make the output current zero when the pipette was in the bath. The junction potential was checked after recording from each cell; data were discarded if the potential drifted more than 3 mV. In one experiment, junction potentials were measured with a low-resistance 3 M-KCl pipette in the bath. They did not vary by more than 1 mV as the bath was perfused with the various test solutions. We did not correct for this error.

After the pipette tip touched a cell, a gigohm seal was formed between the pipette and cell membrane by the application of gentle suction. The resistance from the pipette to ground, due to the parallel resistance of the seal and the patch of membrane that covered the pipette opening, ranged from 40 to 343 GΩ and averaged 161 ± 70 GΩ ($n = 44$). The resistance of the seal alone must have been higher. Once a seal was formed, we waited 3 min to allow the solution in the tip of the pipette to re-equilibrate with the solution in the shaft of the pipette. During this time, capacitive current across the wall of the pipette was electronically cancelled (Fig. 1*A* and *B*). Suction was then applied to rupture the membrane under the pipette tip. After a patch was ruptured, a step of voltage produced a large, transient current due to the charging of the inner segment membrane capacitance, C_m, and a smaller steady current due to the membrane resistance, R_m (Fig. 1*C*). The membrane capacitance was measured by numerically integrating the transient current and dividing by the amplitude of the voltage step. The membrane resistance was measured by dividing the increment in voltage by the increment in steady-state current. Because the seal resistance was much larger than R_m, current passing across the seal resistance could be neglected.

The resistance of the pipette, R_s, was measured by two methods: (i) the amplitude of the voltage step was divided by the peak current recorded at the onset of the capacitive transient

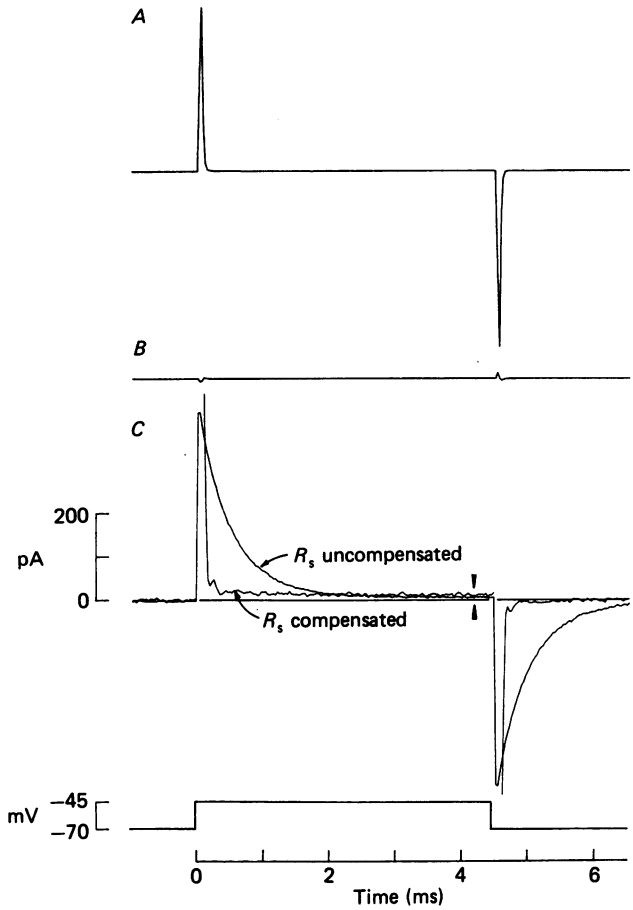

Fig. 1. Compensation for the capacitance and resistance of the pipette. *A*, after a pipette was sealed to the surface membrane, a 25 mV step elicited a transient current due to the pipette capacitance. *B*, a transient current of opposite polarity was injected into the input of the amplifier to cancel the capacitive current at the onset and offset of the voltage step. *C*, after rupturing the patch of membrane beneath the tip of the pipette, the voltage step produced a new transient due to the inner segment membrane capitance, C_m. This transient can be fitted with a single exponential of 0·48 ms time constant. The membrane capacitance calculated by integrating the transient and dividing by the voltage step was 8·6 pF. The series resistance of the pipette, R_s, measured (i) by dividing the amplitude of the voltage step by the peak current recorded at the onset of the transient or (ii) by dividing the time constant of the transient by the membrane capacitance, was 55 MΩ. Compensation for approximately 90% of the series resistance shortened the duration of the transient allowing the current to reach a steady level after 0·2 ms. The recording was low-pass filtered at 30 kHz.

($R_s = \Delta V/\Delta I$) and (ii) the time constant of the transient, τ, was divided by the membrane capacitance ($R_s = \tau/C_m$). These values usually agreed within 1% and, with solutions E and F in the pipette, were typically 30–80 MΩ. This resistance is greater than the 15–35 MΩ measured before a pipette touched an inner segment. The difference suggests that the tip was often partially occluded by cytoplasmic debris. For ramp stimuli (Figs. 2, 3 and 5), the voltage error due to the series resistance was calculated and the recorded command voltage subsequently corrected during data

analysis by subtracting the voltage error point by point. During experiments in which the voltage was stepped to several levels, speed and accuracy were improved by electronically compensating for the series resistance (Hodgkin, Huxley & Katz, 1952). Approximately 90% of the measured series resistance was compensated by adding to the command voltage a signal proportional to the injected current. As Ca currents rarely exceeded 100 pA, the voltage error after compensation was less than 1 mV. With optimum compensation, the capacitive current, and thus the change in membrane potential, was complete 0·2–0·5 ms after initiating a voltage step (Fig. 1*C*). Linear capacitive and resistive currents flowing through the inner segment membrane were measured during a step from −70 to −45 mV, a voltage range in which the Ca current did not activate. They were then scaled and subtracted from currents recorded during larger voltage steps (Figs. 4, 5, 7 and 8).

Stimuli were generated and responses recorded by a computer. Data were low-pass filtered at 20 kHz (for experiments measuring the kinetics of activation and deactivation) or 1 kHz (all other experiments) with an 8-pole, low-pass Bessel filter before being recorded by the computer. Data were additionally filtered during subsequent analysis as specified in each Figure legend. When data were compared with a calculated curve, both were filtered to the same extent.

RESULTS

The calcium current was studied after permeant ions other than Ca were removed from both the internal and external solutions. A procedure for isolating the Ca current is illustrated in Fig. 2. A pipette (filled with solution E) was sealed to the surface of an inner segment; the patch of membrane occluded by the pipette was ruptured; and shortly thereafter the external solution was changed from the physiological saline (solution A) to a medium lacking permeant monovalent ions (solution B). During the next 1–2 min the diffusible components of the cytoplasm exchanged with the solution within the pipette and the new external solution washed into the chamber. Current–voltage curves were measured at 3 s intervals by changing the voltage from −70 to +50 mV at the constant rate of 156 mV/s (Fig. 2*A*). Current–voltage curves measured in this way do not indicate steady-state behaviour if a current activates slowly. Nonetheless, the method was convenient for observing qualitative changes in total membrane current after initiating a change in the internal and external solutions. As permeant ions other than Ca were depleted, the current–voltage curve changed. After approximately 2 min an inward current remained. It activated at approximately −35 mV, reached a maximum at approximately 0 mV, and then declined with further depolarization. Two observations indicate that the current was carried by Ca. First, the current was rapidly and reversibly blocked when Ca in the external medium was replaced by Co (Fig. 2*B*). Secondly, the amplitude of the current was increased 10–20% when Ca was replaced with Ba.

Membrane resistivity

The membrane resistance, R_m, measured between −70 and −45 mV from the curve illustrated in Fig. 2 that was recorded 10 s after rupturing the patch is 2·4 GΩ (average value for twenty-three cells, 2·1 ± 1·3 GΩ, mean ± S.D.), a value similar to the 2·1 ± 0·5 GΩ observed by Bader *et al.* (1982). In comparison, the resistance from the pipette to ground before rupturing the patch was 75 GΩ. Thus, the seal of the pipette against the membrane was not a significant shunt and the measured resistance was due almost entirely to membrane properties. The inner segment capacitance, C_m, was 14·1 pF (average of twenty-three cells; 12·5 ± 3·6 pF). If a specific membrane

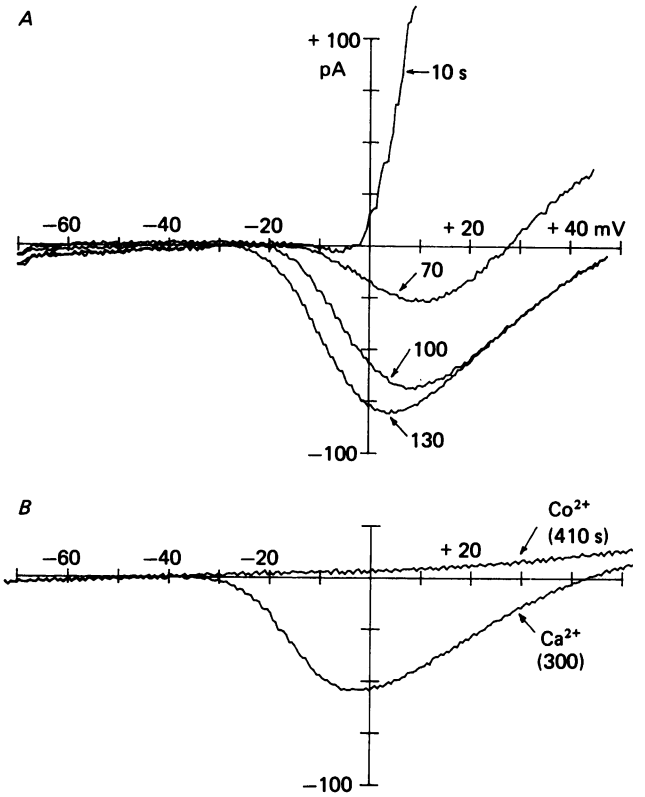

Fig. 2. Isolation of the Ca current. *A*, current–voltage curves from an inner segment generated by a command voltage that increased from −70 to +50 mV at 156 mV/s. The pipette contained solution E. Curves were measured at the time indicated after rupturing the patch and changing the external medium from a physiological saline (solution A) to a medium containing only Ca as a permeant ion (solution B). *B*, selective block of the Ca current by changing from solution B to a medium lacking Ca and containing Co (solution C). Temperature 9·9 °C; the recording was low-pass filtered at 100 Hz; R_m = 2·4 GΩ; C_m = 14·1 pF.

capacitance of 1 μF/cm^2 is assumed, then the specific membrane resistivity with a physiological solution on both sides of the membrane is $3{\cdot}4 \times 10^4$ Ω cm^2. An average value for twenty-three cells was $2{\cdot}7 \pm 1{\cdot}9 \times 10^4$ Ω cm^2.

After the internal and external solutions equilibrated and impermeant monovalent ions were on each side of the membrane, the measured resistance between −70 and −45 mV was 10·2 GΩ (average value for twenty-three cells, 15·2 ± 10·6 GΩ). After the Ca current was blocked with Co or allowed to run down (see below), the resistance decreased when the membrane was depolarized beyond 0 mV (see Fig. 2, trace recorded after 410 s). The non-linear, outward current at +50 mV was 2–15 pA. Voltage steps from −70 to +40 mV with a time resolution of 0·2 ms demonstrated that this current was time independent. We chose for detailed analysis currents recorded from inner segments in which the non-linear, outward current at +50 mV was ten times smaller than the maximum inward Ca current.

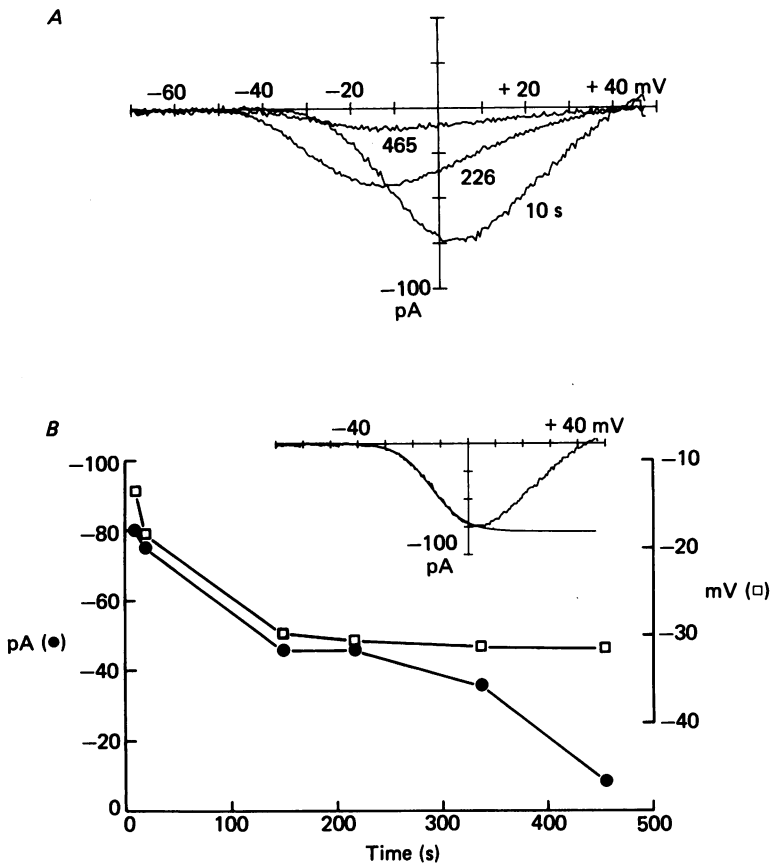

Fig. 3. Run-down and shift in voltage dependence. *A*, the current–voltage curve was measured at intervals after rupturing the patch. The amplitude declined and the potential at which the Ca current activated became more hyperpolarized with time. *B*, the inset shows the curve observed at 10 s fitted with eqn. (1) ($I_{max} = -82$ pA, $A = -13{\cdot}5$ mV, $B = 6{\cdot}0$ mV). Values of I_{max} (scale at left) and A (scale at right) are plotted as a function of time after rupturing the patch. B remained constant. The pipette contained solution E; the external medium was solution D. Linear resistive and capacitive currents were subtracted during data analysis. Temperature 23·7 °C; the recording was low-pass filtered at 1 kHz; $R_m = 30{\cdot}3$ GΩ; $C_m = 9{\cdot}2$ pF.

Run-down and shift in voltage dependence

After the Ca current was isolated, there was a slow change in its amplitude and the voltage range over which it activated. Both changes can be seen in Fig. 2. The current became larger between 100 and 130 s and then smaller by 300 s; the initial increase in amplitude was not always seen; the later decline always occurred. During the same period, depolarization from −70 mV activated the current first at −20 mV (100 s), then −30 mV (130 s), and finally −35 mV (300 s).

In other experiments (an example is illustrated in Fig. 3) the Ca current was isolated as quickly as possible by continuously bathing inner segments in a solution in which Ca was the only permeant ion (solution B). At 10 s after rupturing the patch,

the current was predominantly inward. Between 10 and 226 s the peak amplitude decreased and the voltage at which the current activated shifted to a more hyperpolarized potential. Between 226 and 465 s the amplitude continued to decrease but without an additional shift in the activation potential.

A description of the change in voltage dependence and amplitude was made by fitting a sigmoid curve to the increasing portion of the current–voltage relation (Fig. 3*B*, inset), using the function

$$I = I_{max}(1 + \exp((A - V)/B))^{-1}, \quad (1)$$

where I is the current at voltage V; I_{max} is the maximum value of the steady-state current; A is the voltage at which the sigmoid is half-maximum and B is a constant that determines how steeply the current increases as voltage is changed. In nine inner segments A shifted from -22 ± 6 mV to -31 ± 6 mV (mean $\pm$ S.D.). The initial value, -22 mV, is the same as the value calculated from the data reported by Bader *et al.* (1982). B was $4{\cdot}3 \pm 0{\cdot}6$ mV, slightly smaller than the value of 5·3 mV calculated from their data. In each inner segment the voltage sensitivity B did not change by more than 0·1 mV during the shift, suggesting that the mechanism causing the shift acts simultaneously on all channels. If there was a discrete modification of the voltage sensitivity of individual channels, we would expect to see first a broadening of the curve as a portion of the channels became modified, and then a return to the original steepness after all channels had been modified. Values of I_{max} and A are plotted in Fig. 3*B*. The shift in the activation voltage was usually completed by 150 s; the decline in amplitude usually continued during the entire period of recording. There did not appear to be a simple relationship between these two phenomena.

Marty & Neher (1983) have observed a shift in the voltage dependence of macroscopic Na currents during recording from chromaffin cells. They have attributed the shift to an alteration in junction potential produced by cytoplasmic anions which hold the interior of the cell more negative than the pipette. After rupturing a patch these anions are thought to diffuse from the cell. The current–voltage curve would simultaneously shift to more negative potentials. This mechanism predicts a maximum shift of 12 mV (Marty & Neher, 1983), less than the 18 mV shift we have occasionally observed (see Fig. 3*B*). Moreover, it predicts a shift of the entire current–voltage curve and does not explain a shift in the curve between -40 and 0 mV without a change in the curve at large positive potentials (compare the curves measured at 100 and 130 s in Fig. 2*A*). The shift we have observed acts more like a change in the voltage dependence of Ca channels than like a change in junction potential. It could be due to a change in surface potential at the inner surface of the membrane which occurs as intracellular ions are changed.

Ca currents have been observed previously to disappear slowly when cytoplasm is exchanged or dialysed (Kostyuk, Krishtal & Pidoplichko, 1981; Byerly & Hagiwara, 1982; Fenwick, Marty & Neher, 1982). This consistent observation in a variety of cells has given rise to the notion that the integrity of a Ca current depends upon soluble cytoplasmic factor(s) that are lost during exchange. For this reason the phenomenon has been termed 'run-down' or 'wash-out'. Attempts have been made to supplement the internal solution in order to replace the lost factor(s). Cyclic AMP has been reported to slow the rate of disappearance of some Ca currents (Fedulova, Kostyuk & Veselovsky, 1981; Doroshenko, Kostyuk & Martynyuk, 1982; Irisawa &

Kokubun, 1983). In early experiments, we added cyclic AMP (50 μM), ATP (2 mM), and GTP (0·2 mM), either individually or together, to the solution in the pipette. These additions had no obvious effect on the rate of the disappearance observed in inner segments and, therefore, were not used in subsequent experiments.

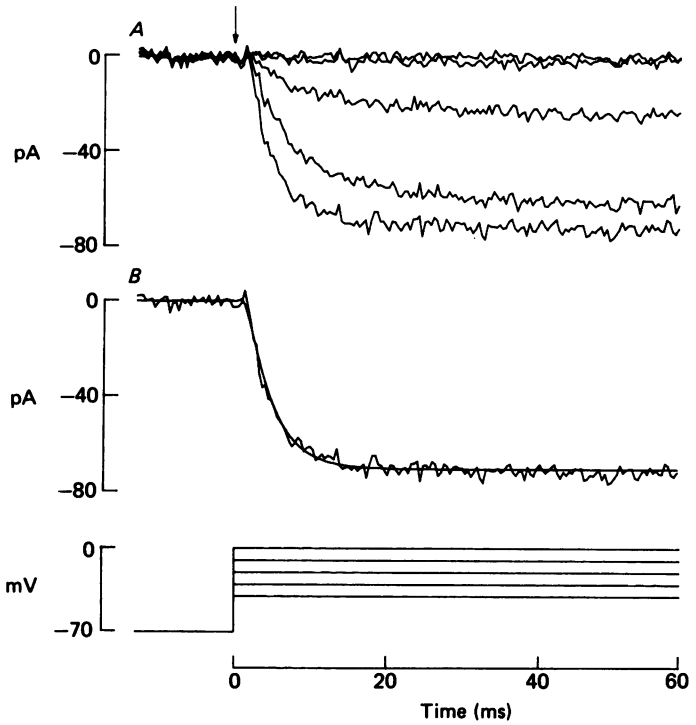

Fig. 4. Activation of the Ca current. *A*, superimposed are Ca currents observed during steps from −70 mV to −40, −30, −20, −10 and 0 mV as indicated in the bottom traces. Linear capacitive and resistive components were measured between −70 and −45 mV, scaled, and subtracted from each original record to yield the Ca currents alone. The arrow indicates the time of onset of the voltage steps. There is an apparent delay of approximately 1·2 ms before the current begins to increase. *B*, the Ca current observed during a step from −70 to 0 mV is compared with a curve calculated as the sum of two exponentials, one of +44 amplitude and 1·0 ms time constant and a second of −118 pA amplitude and 3·3 ms time constant. External medium solution B; pipette contained solution E; temperature 10·2 °C; the recording was low-pass filtered at 10 kHz; R_m = 3·2 GΩ; C_m = 11·1 pF.

Two methods of measuring the steady-state current–voltage relation

The steady-state current–voltage relation for the Ca current was obtained by stepping the voltage from −70 mV to various depolarized potentials and measuring the current after it had reached a steady level (Fig. 4*A*). The results from the cell of Fig. 4 are plotted against membrane potential in Fig. 5 *A* (filled squares). For comparison, the current–voltage curve obtained by ramping the voltage from −70 to +50 mV is also shown. The two agree because activation of the Ca current was rapid compared to the speed of the ramp and no inactivation occurred when the internal Ca concentration was buffered by 10 mM-EGTA (see below). Hence, both procedures measured the steady-state current–voltage relation.

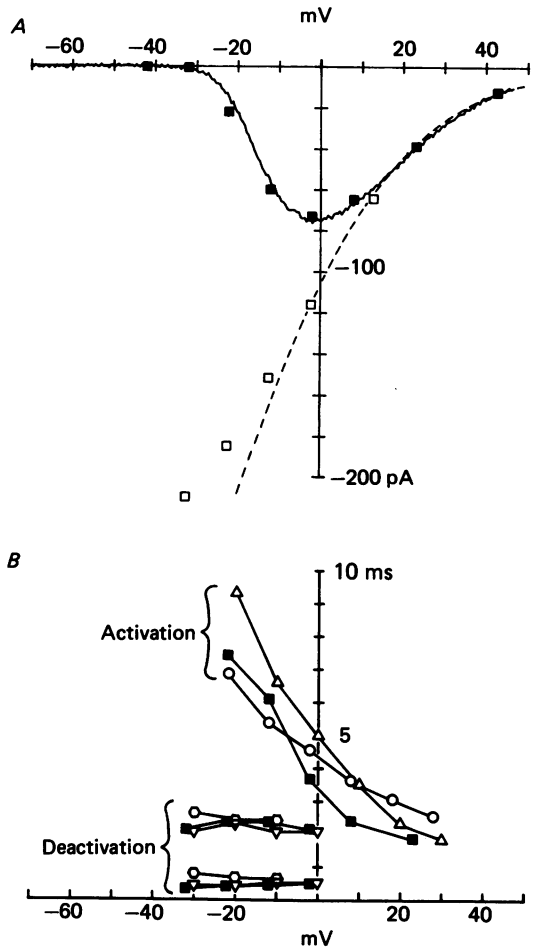

Fig. 5. Voltage dependence of the Ca current. *A*, the current–voltage curve measured by changing the voltage from −70 to +50 mV at 156 mV/s is compared with the relation measured at the end of 60 ms steps (filled squares; data from the records of Fig. 4). The current–voltage relation for the fully activated Ca conductance was measured by first depolarizing to +15 mV and then repolarizing to one of several test potentials (open squares; data from records of Fig. 6). Because the current was measured 0·5 ms after repolarization, the points underestimate the true relation. The dashed line is the prediction of eqn. (2) with $z^2F^2P[\mathrm{Ca}]_o/RT = 8{\cdot}3$ nS. *B*, the slower time constant for activation and both time constants for deactivation are plotted for this cell and two additional cells as functions of membrane potential. Temperature between 10·0 and 10·7 °C; the pipette was filled with solution E; the bath contained solution D (hexagons) or solution B (all others).

Instantaneous current–voltage relation

The steady-state current–voltage relation (Fig. 5*A*, filled squares) is determined by the product of the current passing through an open Ca channel and the probability that a channel is open. The voltage dependence of the current through open channels can be estimated by first opening channels, then rapidly changing the membrane potential and measuring the current before channels close. An example is shown in

Fig. 6*A*. Channels were first opened by stepping the voltage from −70 to +15 mV. The current was then measured 0·5 ms after changing the voltage to a new level. These values are plotted in Fig. 5*A* by the open squares. If the time required to change the voltage to a new level allowed some channels to close, then the observed values would underestimate the true 'instantaneous' current–voltage relation. Because the membrane potential was not constant during the initial 0·5 ms, we have not attempted to estimate the instantaneous relation by extrapolating the current to earlier times. The observed values can be compared with a curve calculated from the Goldman–Hodgkin–Katz equation (Hodgkin & Katz, 1949; see Hagiwara & Byerly, 1981). If the internal concentration is much less than the external concentration, then

$$I = zPF\xi[\mathrm{Ca}]_0 (1-\mathrm{e}^{\xi})^{-1}, \quad (2)$$

where $\xi = zVF/RT$; z, V, F, R and T have their usual significance; P is a permeability constant; $[\mathrm{Ca}]_0 = 6$ mM. The instantaneous current–voltage relation is roughly described by the Goldman–Hodgkin–Katz equation (dashed line in Fig. 5*A*).

Kinetics of activation and deactivation

The time course for activation of the Ca current was measured during depolarizing steps (Fig. 4). The kinetics were slowed by reducing the temperature to 10 °C. The observed time course can be described with a curve calculated as the sum of two exponentials. In Fig. 4*B*, for example, the response to a step to 0 mV was fitted with a fast exponential component of +44 pA amplitude and 1·0 ms time constant summed with a slow component of −118 pA amplitude and 3·3 ms time constant. The faster and smaller component produces a delayed onset, here about 1·2 ms, but does not affect the shape of the curve beyond the first few milliseconds. The effect of a rapid component would predominate during the initial 0·5 ms, which was also the time when the membrane potential was changing. Accordingly, we were not able to measure this component accurately. The slow component, which represents the rate-limiting process in channel activation, could be measured. Its time constant decreased as the membrane was depolarized, changing from 8 to 2 ms within the voltage range studied (Fig. 5*B*).

The time course for deactivation of the Ca current was measured by first activating the current and then repolarizing. In Fig. 6*A* are superimposed records of Ca currents observed when the membrane was repolarized to three different levels. The kinetics of deactivation can be described by the sum of two exponentials. In Fig. 6*B*, the current following a step from +15 mV to −30 mV is compared with a curve computed from the sum of two exponentials. The slower component has a time constant of 2·3 ms (indicated by the dashed line); the faster and larger component has a time constant of 0·35 ms. Because the fast component was large, it could be measured even after the time required for the voltage clamp to settle (0·4–0·5 ms in this record). The time constants for both components are plotted as a function of voltage in Fig. 5*B*. They are relatively independent of voltage over the range studied.

The data in Fig. 5*B* demonstrate that both time constants for deactivation differ from the slower time constant for activation. Thus, at least three different exponential terms are needed to describe both activation and deactivation at one voltage (the faster time constant for activation may be equal to one of the time constants observed

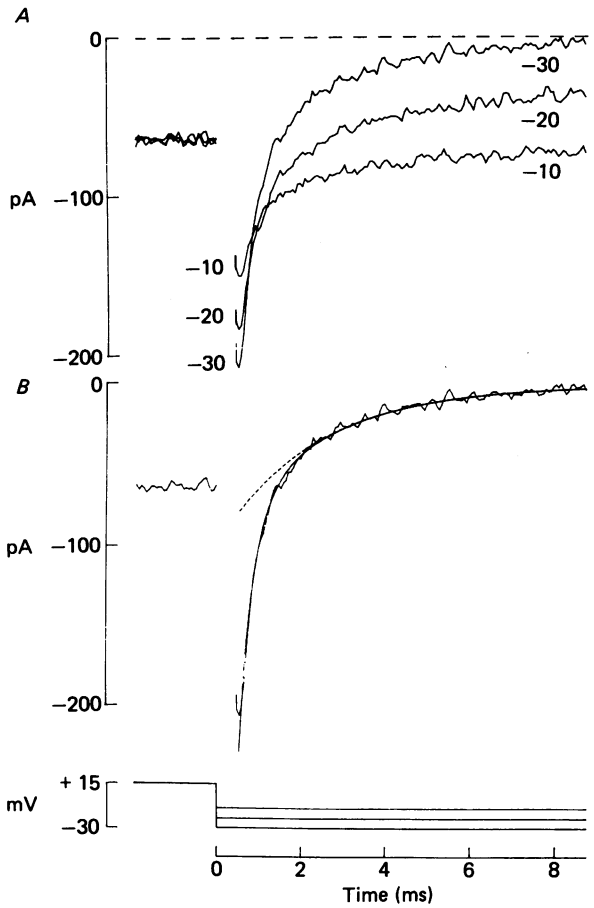

Fig. 6. Deactivation of the Ca current. *A*, superimposed are Ca currents observed during steps from +15 mV to a series of voltages as indicated adjacent to each current trace. Linear capacitive and resistive components were measured between −70 and −45 mV, scaled, and then subtracted from each original record. Subtracting linear capacitive and resistive components from the current recorded during a step between −70 and −115 mV yielded no net current after the 0·4 ms transient was completed (not shown). *B*, the Ca current observed during a step from +15 to −30 mV is compared with a curve calculated as the sum of two exponentials, one of −78 pA amplitude and 2·3 ms time constant and a second of −141 pA amplitude and 0·35 ms time constant. The dashed line is the 2·3 ms exponential alone. Same inner segment as in Fig. 4.

during deactivation). The number of exponential terms is determined by the number of conformational states. If channel molecules can exist in n states, then the solution of $(n-1)$ linear equations containing $(n-1)$ exponential terms will characterize the system. Consequently, three exponential terms indicate that the Ca channel in rod inner segments must have at least four states. The kinetics of the Ca current in snail neurones also indicate a channel with four states (Byerly & Hagiwara, 1982). The kinetics of the current observed in bovine chromaffin cells requires a description with

at least three states and time constants for deactivation that are voltage dependent (Fenwick *et al.* 1982). The differences between Ca currents observed in chromaffin cells by Fenwick *et al.* and in rod inner segments by ourselves are not due to differences in the composition of media used in each study. We have recorded from chromaffin cells with our solutions and procedures and observed kinetics similar to those reported by Fenwick *et al.* (1982).

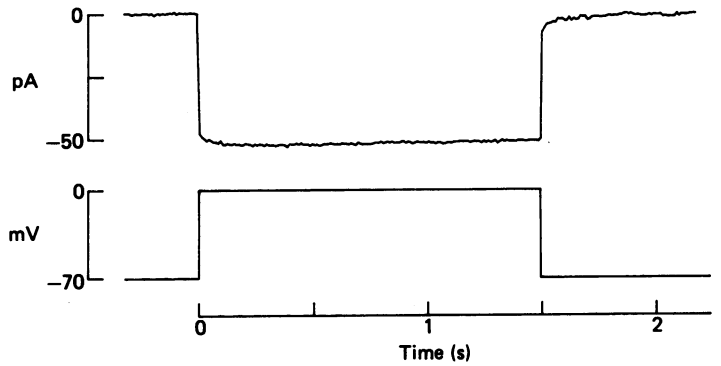

Fig. 7. Absence of voltage-dependent inactivation. The pipette contained 10 mM-EGTA and 0·61 mM-Ca to buffer the internal Ca concentration at 10^{-8} M (solution E). Depolarization from −70 to 0 mV produced a maintained current without evidence of decline for 1·5 s. The large, transient, inward current produced upon repolarization was too brief to be observed on this time scale. External medium was solution B; temperature 21·0 °C; the recording was low-pass filtered at 100 Hz; R_m = 30·1 GΩ; C_m = 16·6 pF.

Inactivation

The Ca conductance in many tissues declines during a maintained depolarization (see reviews by Hagiwara & Byerly, 1981 and Tsien, 1983). In some cases this process of inactivation is controlled directly by voltage (Fox, 1981; see Tsien, 1983). In other cases, inactivation is secondary to an increase in cytoplasmic Ca concentration (Hagiwara & Nakajima, 1966; Kostyuk & Krishtal, 1977; Takahashi & Yoshi, 1978; Brehm, Eckert & Tillotson, 1980; Plant, Standen & Ward, 1983; see Tsien, 1983). We looked first for voltage-dependent inactivation. The internal Ca concentration was buffered with 10 mM-EGTA (solution E). No inactivation was apparent with a depolarizing step of 1·5 s (Fig. 7) or even 7·5 s duration. Consequently, if voltage-mediated inactivation can occur, it must proceed with a time constant slower than 30 s at a temperature of 22 °C. Bader *et al.* (1982) have previously demonstrated that voltage-mediated inactivation must proceed with a time constant slower than approximately 3 s. The present finding extends the time scale tenfold.

We studied Ca-dependent inactivation by lowering the EGTA concentration in the pipette a hundredfold. Ca influx could then raise the internal Ca concentration. When the Ca current was recorded with a pipette containing 0·1 mM-EGTA (solution F), a step to 0 mV evoked a Ca current which appeared to decline with time (Fig. 8). A similar decline was never observed when the pipette contained 10 mM-EGTA (solution E). The apparent decline may be due to inactivation of the inward Ca

current or to the slow appearance of an outward, Ca-activated current. Two Ca-activated conductances exist in rod inner segments (Bader *et al.* 1982). We attempted to minimize their influence by replacing the permeant ions in the internal and external solutions with large, relatively impermeant ions. Nonetheless, we could not be certain that permeant ions had been completely replaced and that residual

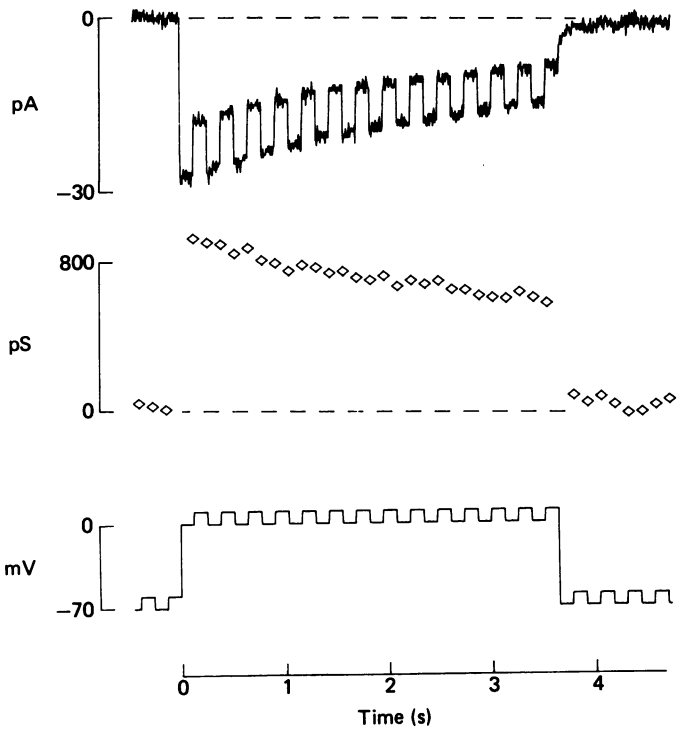

Fig. 8. Ca-mediated inactivation. The pipette contained 0·1 mM-EGTA and no added Ca (solution F). Membrane potential was stepped from −70 to 0 mV. Test pulses (10 mV) were continuously superimposed (bottom trace). The current (upper trace) declined steadily during the 3·6 s step. In the middle is plotted the slope conductance, g_{sl}, calculated from the current change induced by each test pulse ($g_{sl} = \Delta I/\Delta V$). Temperature 23·0 °C. The recording was low-pass filtered at 1 kHz; R_m = 16·8 GΩ; C_m = 11·0 pF.

trace quantities did not distort the result. Therefore, we measured the membrane conductance during the test step. If the Ca current inactivates, conductance would decrease; if an outward Ca-activated current should appear, the conductance would increase. Conductance was measured by superimposing 10 mV test pulses on a depolarizing step to 0 mV (Fig. 8), a potential at which the Ca conductance of the cell illustrated was expected to be fully activated. Consequently, slope conductance should be proportional to the number of open channels. The conductance calculated from the test pulses (middle trace in Fig. 8) declined during the step, indicating that the decrease in the current was due to a true inactivation.

The extent of inactivation depended upon the size of the initial Ca current. When the current was initially larger than 50 pA, a decline in the current occurred during several seconds of depolarization and Ca entry. A smaller decline was produced either by a smaller depolarization (and a smaller Ca current) or by depolarization to the same level after run-down had decreased the maximum size of the current. No inactivation was observed in inner segments when the current was smaller than 10 pA. Thus, an apparent inactivation was incomplete, took seconds to develop and only occurred when the current was larger than might be expected to occur during physiological conditions (see Discussion).

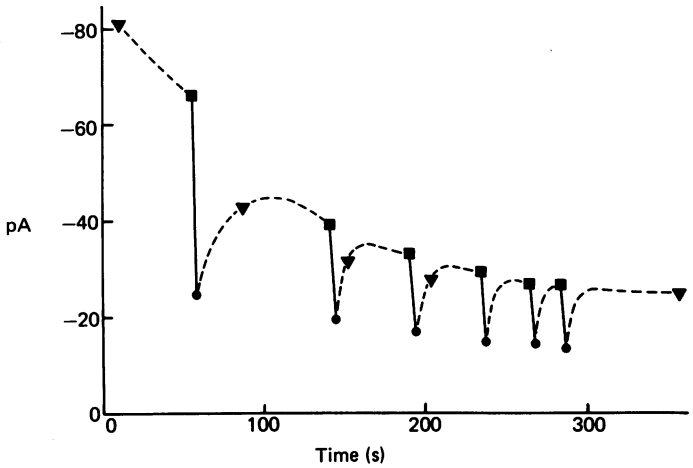

Fig. 9. Inactivation superimposed on run-down. The amplitude of the Ca current measured at 0 mV by either a ramp (triangles) or a step to 0 mV is plotted as a function of time after rupturing the patch. During each step the initial current (squares) declined (as indicated by the continuous lines) to a smaller value (circles). The dashed line has been drawn to indicate the change in current amplitude. Same cell as in Fig. 8, where the record is the fourth in the series shown here.

Inactivation was distinct from run-down. While inactivation was reversible, the continuous disappearance of the current during run-down was irreversible. A comparison is shown in Fig. 9. The Ca current was measured at 0 mV either by a ramp (triangles) or during a 3·5 s step. During each step the current activated to a maximum (squares) and then slowly declined (continuous lines) to a smaller value (circles). The process of inactivation that occurs during each step appears to be superimposed on a continuous, irreversible disappearance. Although episodes of Ca accumulation may speed run-down (Byerly & Hagiwara, 1982; Fenwick *et al.* 1982), the preceding experiment indicates that inactivation and run-down are distinct processes. This is also indicated by the observation that it was possible to prevent inactivation by buffering the internal Ca concentration (as described above) but not possible to prevent run-down.

DISCUSSION

Light initiates in the rod outer segment a transient hyperpolarization which spreads to the inner segment to control Ca channels and alter the release of transmitter. The time constants for changes in state of Ca channels are faster than the membrane time constant and much faster than the kinetics of the response to light. The Ca current deactivates during the initial hyperpolarization and reactivates during the subsequent depolarization. Consequently, in the absence of inactivation, changes in the Ca current mirror the change in voltage produced by dim light.

Voltage-mediated inactivation, if it occurs, must have a time constant longer than 30 s (see Fig. 7 and text). Ca-mediated inactivation did not occur when the current was smaller than 10 pA. During darkness, rods are depolarized to between −40 and −35 mV; during light, their membrane potential is increased. The Ca current is activated at voltages more depolarized than −40 mV (Figs. 2, 3 and 5). Consequently, the range of intracellular potentials that can be produced by light has only a small overlap with the range of voltages in which the Ca current is activated. Therefore, it seems unlikely that the Ca current could ever be more than a few picoamperes during physiological conditions. Thus inactivation probably does not modify the Ca current during the response to a flash of light.

Intuitively, it may seem desirable for membrane voltage to have a large effect on Ca influx and transmitter release. This would happen if the membrane potential of a dark-adapted rod were near the voltage at which the current was half-maximum: −22 mV. Instead, the membrane potential lies in a range where the ability of voltage to control Ca influx is reduced twentyfold (the derivative of eqn. (1) with $I_{max} = -100$ pA, $A = -22$ mV, and $B = 4{\cdot}3$ mV predicts that the Ca current would change 6·25 pA/mV at −22 mV and 0·35 pA/mV at −35 mV). Ca-activated currents prevent the Ca current from becoming very large. Depolarization increases the Ca current which in turn initiates two Ca-activated currents. These are more than sufficient to oppose further depolarization (see Bader *et al.* 1982, Fig. 19). The Ca current and Ca-activated currents create a feed-back system that acts to maintain the voltage within a narrow range at the 'foot' of the Ca current–voltage curve. Weak currents can displace the voltage momentarily, but after a few hundred milliseconds the balance of Ca and Ca-activated currents re-adjusts to return the membrane towards the original voltage. Thus a low level of Ca influx and transmitter release are maintained in the dark. A small hyperpolarization by light reduces Ca influx and Ca-dependent synaptic transmission.

Photoreceptors have two morphological types of synapse (see discussion in Miller & Schwartz, 1983). Invaginating junctions, contacting bipolar and horizontal cells, release transmitter by Ca-dependent exocytosis. Basal junctions, contacting only certain bipolar cells, have been suggested to release transmitter by a Ca-independent mechanism (Miller & Schwartz, 1983). Recent experiments indicate that the Ca-dependent transmission from rods to horizontal cells only operates over a few millivolts of presynaptic polarization. The limited range of voltage which controls transmission to horizontal cells corresponds to the limited range of voltage in which the Ca current is activated. The similarity indicates that the Ca current which we have studied could regulate exocytosis.

One absorbed photon transiently decreases the phototransduction current entering the outer segment by approximately 1 % or 0·5 pA (Baylor, Lamb & Yau, 1979). Electrical coupling between rods (Schwartz, 1973, 1975, 1976; Fain, Gold & Dowling, 1976; Copenhagen & Owen, 1976; Leeper, Norman & Copenhagen, 1978; Detwiler, Hodgkin & McNaughton, 1980; Griff & Pinto, 1981) allows this current change to spread to neighbouring rods. Because of coupling, the rod that absorbs a photon produces a voltage that is ten to fourteen times smaller than if rods were not coupled. The 30 μV hyperpolarization produced by one absorbed photon (Schwartz, 1975; Copenhagen & Owen, 1976) could (using eqn. (1)) stop approximately 0·01 pA of the 1·4 pA Ca current present during darkness. The magnitude of the current stopped is of the same order of magnitude as the current through a single Ca channel (see Tsien, 1983). Of course, a single channel is open only a brief time, approximately 1 ms (Reuter, Stevens, Tsien & Yellen, 1982; Fenwick *et al.* 1982; Hagiwara & Ohmori, 1983), and the response to one photon lasts approximately 1–2 s. Therefore, the absorption of one photon closes approximately 10^3 Ca channels in the 'illuminated' rod during the time course of the light response. Put another way, a single photon ultimately decreases Ca influx 0·7 % by stopping 3×10^4 Ca ions from entering the illuminated rod. For comparison, a free cytoplasmic concentration of 0·1 μM in a 4 pl volume would correspond to $2{\cdot}4 \times 10^5$ ions.

Our study was begun during the Single Channel Recording Course of 1981 at Cold Spring Harbor Laboratory. The research described was supported in part by a Muscular Dystrophy Association post-doctoral fellowship, NIH Research Grant EY-04526, and a grant from the National Society to Prevent Blindness (to D. P. Corey); National Science Foundation Grant BNS 79-21505 and MH-14277 (to G. Oxford); NIH Research Grant EY-02440 (to E. A. Schwartz); and NIH Research Grant NS-12961 (to C. F. Stevens).

REFERENCES

ASHMORE, J. F. & FALK, G. (1980). The single-photon signal in rod bipolar cells of the dogfish retina. *Journal of Physiology* **300**, 151–166.

BADER, C. R., MACLEISH, P. R. & SCHWARTZ, E. A. (1978). Responses to light of solitary rod photoreceptors isolated from the salamander retina. *Proceedings of the National Academy of Sciences of the U.S.A.* **75**, 3507–3511.

BADER, C. R., BERTRAND, D. & SCHWARTZ, E. A. (1982). Voltage-activated and calcium-activated currents studied in solitary rod inner segments from the salamander retina. *Journal of Physiology* **331**, 253–284.

BAYLOR, D. A., LAMB, T. D. & YAU, K.-W. (1979). Responses of retinal rods to single photons. *Journal of Physiology* **288**, 613–634.

BREHM, P., ECKERT, R. & TILLOTSON, D. (1980). Calcium-mediated inactivation of calcium current in *Paramecium*. *Journal of Physiology* **306**, 193–203.

BYERLY, L. & HAGIWARA, S. (1982). Calcium currents in internally perfused nerve cell bodies of *Limnea stagnalis*. *Journal of Physiology* **322**, 503–528.

COPENHAGEN, D. R. & OWEN, W. G. (1976). Functional characteristics of lateral interactions between rods in the retina of the snapping turtle. *Journal of Physiology* **259**, 251–282.

COREY, D. P. & STEVENS, C. F. (1983). Science and technology of patch-recording electrodes. In *Single-Channel Recording*, ed. SAKMANN, B. & NEHER, E., pp. 53–68. New York: Plenum Press.

DETWILER, P. B., HODGKIN, A. L. & MCNAUGHTON, P. A. (1980). Temporal and spatial characteristics of the voltage response of rods in the retina of the snapping turtle. *Journal of Physiology* **300**, 213–250.

DOROSHENKO, P. A., KOSTYUK, P. G. & MARTYNYUK, A. E. (1982). Intracellular metabolism of adenosine-3′,5′-cyclic monophosphate and calcium inward current in perfused neurones of *Helix pomatia*. *Neuroscience* **7**, 2125–2134.

FAIN, G. L., GOLD, G. H. & DOWLING, J. E. (1976). Receptor coupling in the toad retina. *Cold Spring Harbor Symposia on Quantitative Biology* **40**, 547–561.

FEDULOVA, S. A., KOSTYUK, P. G. & VESELOVSKY, N. S. (1981). Calcium channels in the somatic membrane of the rat dorsal root ganglion neurons, effect of cAMP. *Brain Research* **214**, 210–214.

FENWICK, E. M., MARTY, A. & NEHER, E. (1982). Sodium and calcium channels in bovine chromaffin cells. *Journal of Physiology* **331**, 599–635.

FOX, A. P. (1981). Voltage-dependent inactivation of a calcium channel. *Proceedings of the National Academy of Sciences of the U.S.A.* **78**, 953–956.

GRIFF, E. R. & PINTO, L. H. (1981). Interactions among rods in the isolated retina of *Bufo marinus*. *Journal of Physiology* **314**, 237–254.

HAGIWARA, S. & BYERLY, L. (1981). Calcium channel. *Annual Review of Neuroscience* **4**, 69–125.

HAGIWARA, S. & NAKAJIMA, S. (1966). Effects of the intracellular Ca ion concentration upon the excitability of the muscle fiber membrane of a barnacle. *Journal of General Physiology* **49**, 807–818.

HAGIWARA, S. & OHMORI, H. (1983). Studies of single calcium channel currents in rat clonal pituitary cells. *Journal of Physiology* **336**, 649–661.

HAMILL, O. P., MARTY, A., NEHER, E., SAKMANN, B. & SIGWORTH, F. J. (1981). Improved patch-clamp techniques for high-resolution current recording from cells and cell-free membrane patches. *Pflügers Archiv*, **391**, 85–100.

HECHT, S., SHLAER, S. & PIRENNE, M. H. (1942). Energy, quanta, and vision. *Journal of General Physiology* **25**, 819–840.

HODGKIN, A. L., HUXLEY, A. F. & KATZ, B. (1952). Measurement of current–voltage relations in the membrane of the giant axon of *Loligo*. *Journal of Physiology* **116**, 424–448.

HODGKIN, A. L. & KATZ, B. (1949). The effect of sodium ions on the electrical activity of the giant axon of the squid. *Journal of Physiology* **108**, 37–77.

IRISAWA, H. & KOKUBUN, S. (1983). Modulation by intracellular ATP and cyclic AMP of the slow inward current in isolated single ventricular cells of the guinea-pig. *Journal of Physiology* **338**, 321–337.

KOSTYUK, P. G. & KRISHTAL, O. A. (1977). Effects of calcium and calcium-chelating agents on the inward and outward current in the membrane of mollusc neurones. *Journal of Physiology* **270**, 569–580.

KOSTYUK, P. G., KRISHTAL, O. A. & PIDOPLICHKO, V. I. (1981). Calcium inward current and related charge movements in the membrane of snail neurones. *Journal of Physiology* **310**, 403–421.

LEEPER, H. F., NORMANN, R. A. & COPENHAGEN, D. R. (1978). Evidence for passive electronic interactions in red rods of toad retina. *Nature* **275**, 234–236.

MARTY, A. & NEHER, E. (1983). Tight-seal whole-cell recording. In *Single Channel Recording*, ed. SAKMANN, B. & NEHER, E., pp. 107–122. New York: Plenum Press.

MILLER, A. M. & SCHWARTZ, E. A. (1983). Evidence for the identification of synaptic transmitters released by photoreceptors of the toad retina. *Journal of Physiology* **334**, 325–349.

PLANT, T. D., STANDEN, N. B. & WARD, T. A. (1983). The effects of injection of calcium ions and calcium chelators on calcium channel inactivation in *Helix* neurones. *Journal of Physiology* **334**, 189–212.

REUTER, H., STEVENS, C. F., TSIEN, R. W. & YELLEN, G. (1982). Properties of single calcium channels in cardiac cell culture. *Nature* **297**, 501–504.

SCHWARTZ, E. A. (1973). Responses of single rods in the retina of the turtle. *Journal of Physiology* **232**, 503–514.

SCHWARTZ, E. A. (1975). Rod–rod interaction in the retina of the turtle. *Journal of Physiology* **246**, 617–638.

SCHWARTZ, E. A. (1976). Electrical properties of the rod syncytium in the retina of the turtle. *Journal of Physiology* **257**, 379–406.

SCHWARTZ, E. A. (1982). First events in vision: the generation of responses in vertebrate rods. *Journal of Cell Biology* **90**, 271–278.

SILLEN, L. & MARTELL, A. (1971). *Stability Constants*, supplement 1. London: Chemical Society.

TAKAHASHI, K. & YOSHII, M. (1978). Effects of internal free calcium upon the sodium and calcium channels in the tunicate egg analysed by the internal perfusion technique. *Journal of Physiology* **279**, 519–549.

TSIEN, R. W. (1983). Calcium channels in excitable cell membranes. *Annual Review of Physiology* **45**, 341–358.